Mixed Convection Flow Along a Horizontal Circular Cylinder with Small Amplitude Oscillation in Surface Temperature and Free Stream

Md. Kamrujjaman[1], Md. Anwar Hossain[1] & Jahrul Alam[2]

[1] Department of Mathematics, University of Dhaka, Dhaka, Bangladesh

[2] Department of Mathematics and Statistics, Memorial University, Newfoundland, Canada

Correspondence: Md. Kamrujjaman, Department of Mathematics, University of Dhaka, Dhaka, Bangladesh. E-mail: kamrujjaman@gmail.com

Abstract

The problem is considered on mixed convection flow due to the effect of small amplitude oscillations of a viscous incompressible fluid along a horizontal circular cylinder. Direct implicit finite-difference scheme is employed to solve the dimensionless system of partial differential equations. In case of steady flow, the solutions are presented as functions of the curvature parameter X on the entire surface of the cylinder and there is a visual comparison with the existing result. For fluctuating flow, considering Prandtl number, Pr=1.0, the results are shown graphically in terms of amplitude and phase of the Nusselt number for different values of buoyancy parameter λ. Due to the effect of λ and frequency parameter ω, streamlines and isotherms as well as transient shear stress and heat transfer are illustrated in the interplay of study.

Keywords: Mixed convection, circular cylinder, oscillating flow, free stream, buoyancy parameter

1. Introduction

Combined effect of forced and free convection flows are arising in many applications of real life problems. Some instantaneous examples are as follows:

- electronic devices cooled by fans;

- nuclear reactors cooled during emergency shutdown;

- solar central receivers expand to wind current and;

- heat exchangers placed in a low-velocity environment.

These flows are characterized by the buoyancy parameter $\lambda = Gr/Re^n$, a rational of Grashof and Reynolds number with a positive constant n. The parameter λ depends on the flow structure and the heating conditions of the surface, as well as provides the influence of forced convection in comparison with that of free convection. The mixed convection pattern is generally defined by the range $\lambda \in [\lambda_l, \lambda_u]$, where λ_l and λ_u are the lower and the upper bounds of the regime of mixed convection flow, respectively. Outside the mixed convection reign, $\lambda \notin [\lambda_l, \lambda_u]$, the flow is either the pure free convection ($\lambda < \lambda_l$) or the pure forced convection ($\lambda > \lambda_u$).

In the presence of a boundary layer, the theoretical analysis on mixed convection flow around solid bodies was investigated by Acrivos (1966) for values of the local Nusselt number in the limit of the Prandtl number Pr→ 0 or Pr→ ∞. Merkin (1977) considered that the stream is flowing in the upward direction; the flow regime was discussed with respect to the dimensionless parameter λ (with $n = 2$), say the Richardson number $\alpha = g\beta\Delta Ta/U_0^2 = Gr/Re^2$, where U_0 is the free stream velocity. The solutions were obtained for both small and large α, where forced convection effects dominate for small α while free convection for large α. On a horizontal circular cylinder, a mixed convection boundary layer problem was considered by Hossain, Kutubuddin and Pop (1999).

They studied the effect of radiation-conduction interaction when the temperature is constant. Considering variable surface temperature, Aldoss, Ali, and Al-Nimr (1996) investigated the effect of radial magnetic field on the flow of mixed convection from a horizontal circular cylinder. The results were presented using numerical methods of local non-similarity as well as the coordinate perturbation. Merkin (1967) considered the case of natural convection flow from a circular cylinder in viscous fluid to present a solution to this problem for Newtonian fluid using series expansion. A free convection flow from a horizontal cylinder and axi-symmetric bodies of arbitrary contours was investigated by Lin and Chao (1974).

The lineraziation method was considered for the unsteady forced flow system past a circular cylinder with small oscillating amplitude by Lighthill (1954). A similar problem of axi-symmetric body for a long circular cylinder was analyzed in Glauert and Lighthill (1995). Gorla (1979) examined a harmonic motion of stagnation flow on a circular cylinder in case of time dependent fluid dynamics. The solutions were presented for low and high values of the contracted frequency. Hossain, Hussain, and Rees (2001) investigated the buoyancy force in the unsteady free convection flow through a vertical surface. In the presence of the magnetic field, a fluctuating problem with electrically conducting fluid was analyzed along a vertical plate by Hossain, Das, and Pop (1998). Ramachandran, Chen, and Armaly (1988) analyzed the combined (free and forced) flow in 2D contiguous to a vertical surface for arbitrary wall temperature and surface heat flux variations and obtained the similarity solutions. Continuing the identical flow as before at a 2D stagnation point on a horizontal boundary was smeared by Amin and Riley (1995). The studies in this section dealt with the steady flows, but for practical interest there are many unsteady flow problems. The unsteadiness is due to the change in the free stream velocity and/or wall temperature/heat flux or both. Seshadri, Sreeshylan, and Nath (2002) considered the unsteady mixed convection flow in the stagnation point dangling to a vertical flat plate. The boundary layer equations were solved by using an implicit finite-difference method starting from the initial steady state to the final steady state. Recently, Hossain, Kamrujjaman, and Gorla (2009) dealt with the problems encountered in the viscous incompressible fluid flow field at the free convection flow along a long horizontal cylinder when the temperature of the body is oscillating.

Motivated by the previous work of Acrivos (1966), the present study is exploring the problem defined in Merkin (1977), Hossain et al. (1999) in order to investigate the impact of an oscillating flow. The goal of this paper is to comprehend the influence of oscillating surface temperature on combined flow over a horizontal circular cylinder exposed to a vertical external flow. The nonlinear system of partial differential equations is governing the mixed convection steady mean flow and oscillating flow. The presented model is solved numerically by introducing the finite difference primitive variable transformation method. The stationary solutions for the shear stresses and heat transfer are compared with that of Merkin (1977) and Hossain et al. (1999). For fluctuating flow, the results are shown using the terms amplitude-phase and heat transfer for values of X in $[0, \pi]$ radian, where X is the measurement of curvature. The flow patterns in terms of streamlines and isotherms as well as transient shear stress and heat transfer has been shown graphically with effect of the frequency of oscillation, ω, amplitude of oscillation, ε, different values of the mixed convection parameter λ while the Prandtl number is unique.

2. Mathematical Formalism

Let us consider the problem of a two-dimensional unsteady mixed convection boundary layer flow past a circular cylinder for viscous incompressible fluids. The physical structure and the coordinate system for this flow are displayed in Figure 1. We assume that the undisturbed free stream velocity $(1/2)U_\infty$ is directed vertically upward, and is across the horizontal cylinder, where the flow in the outer region of the boundary approaches to $U_\infty \sin(x/R)$. The surface temperature of the cylinder oscillates with small amplitude about a constant mean temperature. The average surface temperature of the cylinder is maintained at ΔT and the ambient temperature of the fluid is assumed to be T_∞.

Due to the unsteady flow, the fundamental boundary layer equations may now be written as follows:

$$\frac{\partial u}{\partial x} + \frac{\partial v}{\partial y} = 0 \tag{1}$$

$$\frac{\partial u}{\partial t} + u\frac{\partial u}{\partial x} + v\frac{\partial u}{\partial y} = \frac{dU_e}{dt} + U_e\frac{dU_e}{dx} + \nu\frac{\partial^2 u}{\partial y^2} + g\beta(T - T_\infty)\sin\left(\frac{x}{R}\right) \tag{2}$$

$$\rho C_p\left(\frac{\partial T}{\partial t} + u\frac{\partial T}{\partial x} + v\frac{\partial T}{\partial y}\right) = \kappa\frac{\partial^2 T}{\partial y^2} \tag{3}$$

where x is the stream wise direction distance whereas y, the range of normal direction, the velocity terms (u, v) are in the (x, y) channels, $U_e(x)$ the external velocity, t the time, ν the kinematic viscosity, T being the temperature
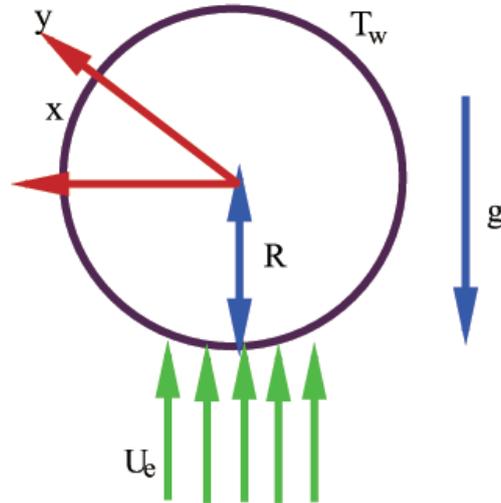
Figure 1. The physical model and coordinate system

of the fluid in the boundary layer, g the gravitational acceleration, β the coefficient of thermal expansion, R the radius of the cylinder, κ the thermal conductivity, ρ the density of the fluid and C_p the specific heat. In momentum equation the pressure gradient term has been written in terms of the outer layer flow and the body force term $g\beta(T - T_\infty)\sin(x/R)$ is due to the buoyancy force under the Boussinesq hypothesis. In fact, U_∞ is the far field velocity, and U_e the outer velocity that is influenced by the oscillating surface temperature.

The boundary conditions for equations (1) to (3) are

$$
\begin{aligned}
y = 0: \quad & u = 0, \quad v = 0, \quad T = T_w(t) \\
y \to \infty: \quad & u \to U_e(x)F(t), \quad T \to T_\infty
\end{aligned}
\tag{4}
$$

In equation (4), $F(t)$ is an oscillating function in t and $U_e(x) = U_\infty \sin(x/R)$ and $T_w(t) = \Delta T F(t)$.

Now we introduce the following non-dimensional quantities

$$
\begin{aligned}
u &= \tfrac{\nu}{R}Re U, \quad v = \tfrac{\nu}{R}Re^{1/2}V, \quad \tfrac{T-T_\infty}{\Delta T} = G \\
Y &= Re^{1/2}\tfrac{y}{R}, \quad X = \tfrac{x}{R}, \quad \tau = \left(\tfrac{\nu}{R^2}Re\right)t
\end{aligned}
\tag{5}
$$

where, $Gr = \frac{g\beta\Delta T}{\nu^2}R^3$, and $Re = \frac{U_\infty R}{\nu}$ are, respectively, the Grashof number and the Reynolds number. Equations (1)-(3) then becomes:

$$
\frac{\partial U}{\partial X} + \frac{\partial V}{\partial Y} = 0
\tag{6}
$$

$$
\frac{\partial U}{\partial \tau} + U\frac{\partial U}{\partial X} + V\frac{\partial U}{\partial Y} = \sin X \cos X + \lambda G \sin X + \frac{\partial^2 U}{\partial Y^2}
\tag{7}
$$

$$
\frac{\partial G}{\partial \tau} + U\frac{\partial G}{\partial X} + V\frac{\partial G}{\partial Y} = \frac{1}{Pr}\frac{\partial^2 G}{\partial Y^2}
\tag{8}
$$

The corresponding boundary conditions are then

$$
\begin{aligned}
Y = 0: \quad & U = 0, \quad V = 0, \quad G = F(\tau) = 1 + \varepsilon \sin(\omega\tau) \\
Y \to \infty: \quad & U \to \sin X(1 + \varepsilon \sin(\omega\tau)), \quad G \to 0
\end{aligned}
\tag{9}
$$

In Equation (9), ω is the frequency of oscillation, $\varepsilon(\ll 1)$ is a positive real number that designates the amplitude of oscillation in surface temperature, τ is the non-dimensional time. Also Pr is known as the Prandtl number and defined to be the ratio of the kinematic viscosity to the thermal diffusivity of the fluid and $\lambda = g\beta\Delta T R/U_\infty^2 = Gr/Re^2$ is a non-dimensional parameter known as mixed convection parameter. For a heated cylinder ($\Delta T > 0$ that implies $\lambda > 0$), both the forced and free convection boundary layers start at the lower stagnation point and

buoyancy force is positive which developed the boundary layer. For a cooled cylinder ($\lambda < 0$) the buoyancy force oppose the development of the boundary layer. In this case, a values of λ is found for which the boundary layer separates at this point and boundary layer solution is not possible less than this values.

For convenience, we further introduce $U = X\bar{U}$ in the above set of equations and obtain the followings by dropping the over bar

$$U + X\frac{\partial U}{\partial X} + \frac{\partial V}{\partial Y} = 0 \tag{10}$$

$$\frac{\partial U}{\partial \tau} + U^2 + XU\frac{\partial U}{\partial X} + V\frac{\partial U}{\partial Y} = \frac{\sin X \cos X}{X} + \lambda\frac{\sin X}{X}G + \frac{\partial^2 U}{\partial Y^2} \tag{11}$$

$$\frac{\partial G}{\partial \tau} + XU\frac{\partial G}{\partial X} + V\frac{\partial G}{\partial Y} = \frac{1}{\Pr}\frac{\partial^2 G}{\partial Y^2} \tag{12}$$

The respective boundary conditions then become as follows:

$$\begin{aligned} Y = 0: \quad & U = 0, \quad V = 0, \quad G = F(\tau) = 1 + \varepsilon\sin(\omega\tau) \\ Y \to \infty: \quad & U \to \frac{\sin X}{X}(1 + \varepsilon\sin(\omega\tau)), \quad G \to 0 \end{aligned} \tag{13}$$

The solution of the above system of differential equations will be obtained in terms of complex functions only, the real parts of which will have physical significance. We write U, V and G as the sum of the steady and small oscillating component as mentioned later in (14). The surface temperature and external velocity conditions in (13) imply the solutions patterns of equations (10)-(12) as defined below

$$\begin{aligned} U(X, Y) &= U_s(X, Y) + \varepsilon\exp(i\omega\tau)U_o(X, Y) \\ V(X, Y) &= V_s(X, Y) + \varepsilon\exp(i\omega\tau)V_o(X, Y) \\ G(X, Y) &= G_s(X, Y) + \varepsilon\exp(i\omega\tau)G_o(X, Y) \end{aligned} \tag{14}$$

where U_s, V_s and G_s represent the steady mean flow satisfying the equations:

$$U_s + X\frac{\partial U_s}{\partial X} + \frac{\partial V_s}{\partial Y} = 0 \tag{15}$$

$$U_s^2 + XU_s\frac{\partial U_s}{\partial X} + V_s\frac{\partial U_s}{\partial Y} = \frac{\sin X \cos X}{X} + \lambda\frac{\sin X}{X}G_s + \frac{\partial^2 U_s}{\partial Y^2} \tag{16}$$

$$XU_s\frac{\partial G_s}{\partial X} + V_s\frac{\partial G_s}{\partial Y} = \frac{1}{\Pr}\frac{\partial^2 G_s}{\partial Y^2} \tag{17}$$

with boundary conditions

$$\begin{aligned} Y = 0: \quad & U_s = 0, \quad V_s = 0, \quad G_s = 1 \\ Y \to \infty: \quad & U_s \to \frac{\sin X}{X}, \quad G_s \to 0 \end{aligned} \tag{18}$$

and for U_o, V_o and G_o, the components of the unsteady flow, are then obtained as

$$U_o + X\frac{\partial U_o}{\partial X} + \frac{\partial V_o}{\partial Y} = 0 \tag{19}$$

$$\begin{aligned} 2U_sU_o + XU_s\frac{\partial U_o}{\partial X} + XU_o\frac{\partial U_s}{\partial X} + V_s\frac{\partial U_o}{\partial Y} + V_o\frac{\partial U_s}{\partial Y} + i\omega U_o \\ = \frac{\sin X \cos X}{X} + \lambda\frac{\sin X}{X}G_o + \frac{\partial^2 U_o}{\partial Y^2} \end{aligned} \tag{20}$$

$$XU_s\frac{\partial G_o}{\partial X} + XU_o\frac{\partial G_s}{\partial X} + V_s\frac{\partial G_o}{\partial Y} + V_o\frac{\partial G_s}{\partial Y} + i\omega G_o = \frac{1}{\Pr}\frac{\partial^2 G_o}{\partial Y^2} \tag{21}$$

Following are the boundary conditions to be satisfied by the above equations

$$\begin{aligned} Y = 0: \quad & U_o = 0, \quad V_o = 0, \quad G_o = 1 \\ Y \to \infty: \quad & U_o \to \frac{\sin X}{X}, \quad G_o \to 0 \end{aligned} \tag{22}$$

3. Method of Solution

We now propose to integrate the set of equations (15)-(17), that represents the steady and the set of equations (19)-(21) representing the oscillatory components of the problem by direct finite difference method. These sets of equations are discretized for numerical scheme using central-difference for diffusion terms and the forward-difference for the convection terms. Thus we have the following system of algebraic equations for the steady state equations:

For the momentum equation, we have

$$A_1(U_s)_{i-1,j} + B_1(U_s)_{i,j} + C_1(U_s)_{i+1,j} = D_1 \tag{23}$$

where

$$A_1 = 1 + \frac{\Delta Y}{2}(V_s)_{i,j}$$

$$B_1 = -2 - (U_s)_{i,j}(\Delta Y)^2 - X_i\frac{(\Delta Y)^2}{\Delta X}((U_s)_{i,j} - (U_s)_{i,j-1})$$

$$C_1 = 1 - \frac{\Delta Y}{2}(V_s)_{i,j}$$

$$D_1 = -(\Delta Y)^2\frac{\sin X_i \cos X_i}{X_i} - \lambda(\Delta Y)^2\frac{\sin X_i}{X_i}(G_s)_{i,j}$$

and $i = 1, 2, 3, \cdots, N$, $j = 1, 2, 3, \cdots, N$ for some large N.

For the energy equation, we obtain

$$A_2(G_s)_{i-1,j} + B_2(G_s)_{i,j} + C_2(G_s)_{i+1,j} = D_2 \tag{24}$$

where

$$A_2 = \frac{1}{\mathrm{Pr}} + \frac{\Delta Y}{2}(V_s)_{i,j}$$

$$B_2 = -\frac{2}{\mathrm{Pr}} - X_i\frac{(\Delta Y)^2}{\Delta X}(U_s)_{i,j}$$

$$C_2 = \frac{1}{\mathrm{Pr}} - \frac{\Delta Y}{2}(V_s)_{i,j}$$

$$D_2 = -\frac{(\Delta Y)^2}{\Delta X}X_i(U_s)_{i,j}(G_s)_{i,j-1}$$

In computation, we directly solve the continuity equation for the normal velocity V_s from the following discretization:

$$\begin{aligned}(V_s)_{i,j} = (V_s)_{i-1,j} + Y_j\frac{1}{4}((U_s)_{i,j} - (U_s)_{i-1,j})\\ - \Delta Y\frac{1}{4}((U_s)_{i,j} + (U_s)_{i-1,j}) - X_i\frac{\Delta Y}{\Delta X}((U_s)_{i,j} - (U_s)_{i-1,j})\end{aligned} \tag{25}$$

The boundary conditions then take the form

$$\begin{aligned}(U_s)_{1,j} = (V_s)_{1,j} = 0, \quad (G_s)_{1,j} = 1\\ (U_s)_{N,j} \to \frac{\sin X_i}{X_i}, \quad (G_s)_{N,j} \to 0\end{aligned} \tag{26}$$

As above we discretize the set of oscillating parts of the solutions posed in equations (20)-(21) as given below:

For the momentum equation, we have

$$A_3(U_o)_{i-1,j} + B_3(U_o)_{i,j} + C_3(U_o)_{i+1,j} = D_3 \tag{27}$$

where

$$A_3 = 1 + \frac{\Delta Y}{2}(V_s)_{i,j}$$

$$B_3 = -2 - (\Delta Y)^2 \left(2(U_s)_{i,j} - \frac{X_i(U_s)_{i,j}}{\Delta X} - X_i \frac{\partial(U_s)_{i,j}}{\partial X}\right)$$

$$C_3 = 1 - \frac{\Delta Y}{2}(V_s)_{i,j}$$

$$D_3 = -(\Delta Y)^2 \left(\frac{\sin X_i \cos X_i}{X_i} + \lambda \frac{\sin X_i}{X_i}(G_o)_{i,j} + \frac{X_i}{\Delta X}(U_s)_{i,j}(U_o)_{i,j-1}\right.$$
$$\left. - (V_o)_{i,j}\frac{\partial(U_s)_{i,j}}{\partial Y} + i\omega(U_o)_{i,j}\right)$$

For the energy equation, we obtain

$$A_4(G_o)_{i-1,j} + B_4(G_o)_{i,j} + C_4(G_o)_{i+1,j} = D_4 \tag{28}$$

where

$$A_4 = \frac{1}{\Pr} + \frac{\Delta Y}{2}(V_s)_{i,j}$$

$$B_4 = -\frac{2}{\Pr} - (\Delta Y)^2 \left(\frac{X_i(U_s)_{i,j}}{\Delta X} - X_i\frac{\partial(G_s)_{i,j}}{\partial X}\right)$$

$$C_4 = \frac{1}{\Pr} - \frac{\Delta Y}{2}(V_s)_{i,j}$$

$$D_4 = -(\Delta Y)^2 \left(\frac{X_i}{\Delta X}(U_s)_{i,j}(G_o)_{i,j-1} - (V_o)_{i,j}\frac{\partial(G_s)_{i,j}}{\partial Y} + i\omega(G_o)_{i,j}\right)$$

As in the previous case we calculate V_o from the following expressions:

$$(V_o)_{i,j} = (V_o)_{i-1,j} + Y_j\frac{1}{4}((U_o)_{i,j} - (U_o)_{i-1,j})$$
$$- \Delta Y\frac{1}{4}((U_o)_{i,j} + (U_o)_{i-1,j}) - X_i\frac{\Delta Y}{\Delta X}((U_o)_{i,j} - (U_o)_{i-1,j}) \tag{29}$$

Appropriate boundary conditions for the above equations are

$$(U_o)_{1,j} = (V_o)_{1,j} = 0, \quad (G_o)_{1,j} = 1$$
$$(U_o)_{N,j} \to \frac{\sin X_i}{X_i}, \quad (G_o)_{N,j} \to 0 \tag{30}$$

The system of equations (23)-(26) and (27)-(30) are transformed to a system of tri-diagonal algebraic equations which have been solved using Gaussian elimination technique for $(U_s)_{i,j}$,
$(G_s)_{i,j}, (V_s)_{i,j}$ and $(U_o)_{i,j}, (G_o)_{i,j}, (V_o)_{i,j}$. The simulation is started at $X = 0.0$, and then out marched to the point $(X = 20.0)$. During the computation, we consider $\Delta X = 0.02$ and $\Delta Y = 0.01$ that are used for the X_i-and Y_j- grids, respectively. For a given value of X, the iterative procedure is ended if the difference in computing the velocity and the temperature in the next iteration is $< 10^{-6}$. Now from the set of equations given in (14), we have the following expressions to measure the dimensionless real part of axial velocity and the temperature functions as given below:

$$U(X, Y, \tau) = U_s(X, Y) + \varepsilon(\cos \omega\tau U_i(X, Y) - \sin \omega\tau U_r(X, Y))$$
$$G(X, Y, \tau) = G_s(X, Y) + \varepsilon(\cos \omega\tau G_i(X, Y) - \sin \omega\tau G_r(X, Y)) \tag{31}$$

In equation (31) U_r, U_i and G_r, G_i are, respectively, the real and imaginary parts of the oscillating velocity function, $U_o(X, Y)$, and the oscillating temperature function, $G_o(X, Y)$. The physical quantities that are important from application point of view are the shear stress, τ_w, and the surface rate of heat transfer, q_w. These can be measured from the non-dimensional relations (32) and (33).

$$\tau_w = X\left[\frac{\partial U_s(X, 0)}{\partial Y} + \varepsilon|A_1|\cos(\omega\tau + \alpha_1)\right] \tag{32}$$

and

$$q_w = -\left[\frac{\partial G_s(X,0)}{\partial Y} + \varepsilon|A_2|\cos(\omega\tau + \alpha_2) \right] \tag{33}$$

Here $|A_1|$ and $|A_2|$ are the amplitudes and α_1 and α_2 are the phase angles, respectively, for the local skin friction and the local heat transfer for the oscillating flow and temperature field which readily available from the following relations:

$$|A_1| = X(\sqrt{(\partial U_r/\partial Y)^2 + (\partial U_i/\partial Y)^2}) \tag{34}$$

$$|A_2| = \sqrt{(\partial G_r/\partial Y)^2 + (\partial G_i/\partial Y)^2} \tag{35}$$

and

$$\alpha_1 = \tan^{-1}\left(\frac{\partial U_i/\partial Y}{\partial U_r/\partial Y}\right) \tag{36}$$

$$\alpha_2 = \tan^{-1}\left(\frac{\partial G_i/\partial Y}{\partial G_r/\partial Y}\right) \tag{37}$$

Once we know the values of and from the solutions of the set (15)-(18) as well as that of and from the solutions of equations (19)-(22), we get readily the values of the physical quantities, namely, the shear stress, τ_w, and the rate of heat transfer, q_w, at the surface of the cylinder.

Numerical values of the amplitudes, $|A_1|$ and $|A_2|$, and the phase-angles, α_1 and α_2, of the oscillating shear-stress and heat transfer rate, respectively, are obtained for different values of the physical parameters, ω, the frequency parameter, Pr, the Prandtl number and λ, the mixed convection parameter, against curvature parameter X. The results presented and discussed in the following section are based on the solution obtained by the method in this section.

Table 1(a): Numerical values of skin-friction $U'_s(X,0)$ for different values of λ while Pr=1.0

X	$\lambda = -1.0$			$\lambda = 0.0$		
	Present DNS	Hossain et al. (1999)	Merkin (1977)	Present DNS	Hossain et al. (1999)	Merkin (1977)
0.0	0.0000	0.0000	0.0000	0.0000	0.0000	0.0000
0.2	0.1254	0.1254	0.1256	0.2422	0.2424	0.2427
0.4	0.2261	0.2255	0.2266	0.4617	0.4618	0.4627
0.6	0.2789	0.2763	0.2784	0.6380	0.6373	0.6393
0.8	0.2554	0.2516	0.2554	0.7541	0.7520	0.7552
1.0	0.1061	0.0985	0.1069	0.7977	0.7936	0.7982
1.2				0.7619	0.7554	0.7615
1.4				0.6446	0.6353	0.6429
1.6				0.4434	0.4309	0.4405
1.8				0.1074	0.0878	0.1069

4. Results and Discussion

The section presents our numerical results that is based on the primitive variable formulation of the direct numerical simulation (DNS). We discuss briefly the flow regime that governs the oscillating mixed convection flow over a heated circular cylinder. The results are summarized with respect to various values of the frequency parameter (ω), the amplitude of oscillation (ε), and the mixed convection parameter (λ). We have chosen a unique value of Prandtl number, Pr=1.0, for most of the results unless it is stated otherwise. The domain of the numerical solution starts from the lower stagnation point of the cylinder and proceeds around the cylinder up to the boundary layer separation point. In order to asses the accuracy of our method, we have compared the surface heat transfer $-G'_s(X,0)$ and the surface shear stress, $U'_s(X,0)$ since experimental data and results from other authors are available for these quantities. The surface heat transfer and the surface shear stress as mentioned above for steady flow are tabulated in Table-1(a,b) and Table-2(a,b) against the curvature parameter X in the interval $[0,\pi]$. The results are

Table 1(b): Numerical values of skin-friction $U'_s(X, 0)$ for different values of λ while Pr=1.0

X	$\lambda = 1.0$			$\lambda = 2.0$		
	Present DNS	Hossain et al. (1999)	Merkin (1977)	Present DNS	Hossain et al. (1999)	Merkin (1977)
0.0	0.0000	0.0000	0.0000	0.0000	0.0000	0.0000
0.2	0.3427	0.3431	0.3436	0.4342	0.4348	0.4354
0.4	0.6621	0.6627	0.6639	0.8440	0.8449	0.8464
0.6	0.9375	0.9374	0.9398	1.2074	1.2079	1.2106
0.8	1.1514	1.1502	1.1539	1.5060	1.5053	1.5094
1.0	1.2919	1.2888	1.2938	1.7263	1.7240	1.7295
1.2	1.3531	1.3478	1.3541	1.8615	1.8569	1.8637
1.4	1.3361	1.3283	1.3356	1.9110	1.9037	1.9117
1.6	1.2481	1.2379	1.2459	1.8769	1.8705	1.8793
1.8	1.0935	1.0902	1.0986	1.7745	1.7689	1.7781
2.0	0.9066	0.9033	0.9117	1.6194	1.6143	1.6236
2.2	0.7020	0.6985	0.7063	1.4295	1.4243	1.4334
2.4	0.5018	0.4978	0.5048	1.2217	1.2163	1.2248
2.6	0.3274	0.3230	0.3287	1.0101	1.0043	1.0123
2.8	0.1985	0.1937	0.1973	0.8028	0.7969	0.8043
3.0	0.1318			0.5992	0.5930	0.6002
π	0.1239			0.4548		

Table 2(a): Numerical values of the rate of heat-transfer $-G'_s(X, 0)$ for different values of λ while Pr=1.0

X	$\lambda = -1.0$			$\lambda = 0.0$		
	Present DNS	Hossain et al. (1999)	Merkin (1977)	Present DNS	Hossain et al. (1999)	Merkin (1977)
0.0	0.5068	0.5066	0.5067	0.5706	0.5704	0.5705
0.2	0.5019	0.5015	0.5018	0.5669	0.5669	0.5668
0.4	0.4867	0.4861	0.4865	0.5562	0.5563	0.5564
0.6	0.4597	0.4588	0.4594	0.5396	0.5388	0.5391
0.8	0.4162	0.4149	0.4160	0.5151	0.5141	0.5145
1.0	0.3315	0.3292	0.3326	0.4832	0.4819	0.4826
1.4				0.3934	0.3914	0.3928
1.8				0.2092	0.2031	0.2114

obtained for different values of the mixed convection parameter $\lambda = -1.0, 0.0, 1.0, 2.0$ when Pr =1.0 and compare with that of Merkin (1967), Hossain et al. (1999). It seems reasonable to conclude that the agreement is acceptable.

The primitive variable transformation method for the internal domain of frequency are engaged in searching the solutions of the system governing the oscillating mixed convection flow along uniformly heated circular cylinders. The foregoing coupled differential equations (20) and (21) together with the boundary conditions (22) have been numerically integrated by the methodology discussed above. It is observed that the unsteady parts of the flow and the temperature fields are dependent on the physical quantities, like the mixed convection parameter λ, the Prandtl number, Pr, the oscillation frequency on the surface temperature, ω, and the amplitude of oscillation, ε. Therefore, simulated results are displayed in terms of amplitude-phase and the heat transfer rate for values of $\lambda = 2.0, 3.0, 5.0, 10.0$ and for fluid having Prandtl number, Pr=1.0. Effects of the aforementioned parameters are discussed in details in the following paragraphs.

4.1 Effect of Physical Parameter on Amplitude and Phase

The numerical values of $(|A_1|, \alpha_1)$ and that of $(|A_2|, \alpha_2)$ for the changing flow are distributed in figures 2-3. Numerical values of $|A_1|$ are depicted in Fig. 2(a) for values of $\lambda = 2.0, 3.0, 5.0, 10.0$ as long as Pr=1.0, $\omega = 0.5$ and $\omega\tau = \pi/4$. It is seen from this figures that the amplitude decreases with increase of X and touches to its

Table 2(b): Numerical values of the rate of heat-transfer $-G'_s(X, 0)$ for different values of λ while Pr=1.0

X	$\lambda = 1.0$			$\lambda = 2.0$		
	Present DNS	Hossain et al. (1999)	Merkin (1977)	Present DNS	Hossain et al. (1999)	Merkin (1977)
0.0	0.6158	0.6156	0.6156	0.6517	0.6516	0.6497
0.2	0.6126	0.6126	0.6115	0.6489	0.6488	0.6471
0.4	0.6036	0.6037	0.6028	0.6407	0.6408	0.6393
0.6	0.5889	0.5891	0.5885	0.6274	0.6276	0.6264
0.8	0.5686	0.5689	0.5686	0.6092	0.6095	0.6086
1.0	0.5431	0.5434	0.5435	0.5865	0.5867	0.5863
1.4	0.4773	0.4776	0.4785	0.5289	0.5290	0.5292
1.8	0.3950	0.3951	0.3967	0.4592	0.4590	0.4601
2.0	0.3490	0.3491	0.3509	0.4215	0.4212	0.4225
2.4	0.2523	0.2520	0.2540	0.3450	0.3444	0.3460
2.8	0.1627	0.1616	0.1634	0.2723	0.2714	0.2730
3.0	0.1357			0.2375	0.2364	0.2381
π	0.1314			0.2125		

minimum point near $X = \pi$ on the cylindrical surface. The nature of this change of curvature is corresponding to that appearing for time independent flow (see Merkin, 1977). Further we see that amplitude of variation increases back to increase in λ. However, the numerical values of the changing phase α_1 of the skin-friction are displayed in Fig. 2(b). Phase angles α_1 in the varying skin friction decrease reaming to increase of λ including the difference of the curvature X. If $\lambda=2.0$ then this trend primarily grows up and for remain numerical values of λ it is reduces with the increase of X and there is a phase lag. In the little frequency domain the result of the integral notice that the periodic term of shear stress reduces in its amplitude with increasing frequency.
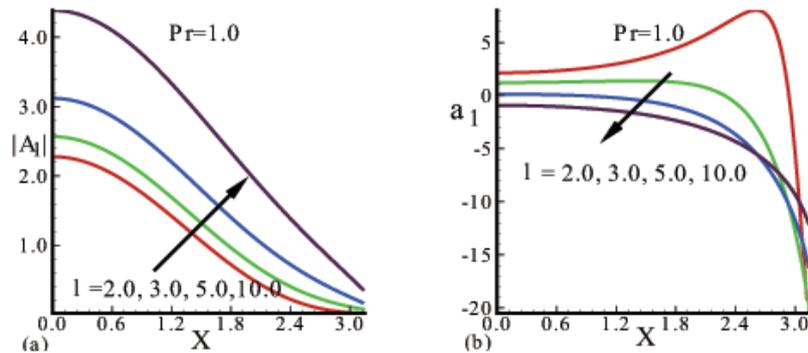

Figure 2. (a) Amplitude and (b) phase of skin-friction at Pr=1.0, $\omega = 0.5$, $\omega\tau = \pi/4$ while $\lambda = 2.0, 3.0, 5.0$ and 10.0.

Figures 3(a) and 3(b) represent the numerical results of the amplitude $|A_2|$ and the phase α_2 respectively, obtained for the fluctuating coefficients of heat transfer for different λ as long as fluids Prandtl number Pr=1.0. It is seen from figure 3(a) that the amplitude $|A_2|$, of the rate of heat transfer increases when the parameter λ is increasing. Amplitude of heat transfer leads to decrease along the surface from its lower point to the upper of the cylinder for any λ. The relative maximum value of the amplitude arises at the lower stagnation point $X = 0$. In figure 3(b) it is observed that phase of oscillation α_2 in the rate of heat transfer are decreases owing to increase of λ untill it reaches to the curvature $X = \pi$. Continually there is a phase lead for parameter λ.

4.2 Effect of Physical Parameter on Streamlines and Isotherms

Now we try to observe the effect of pertinent physical parameters, such as, λ and ω controlling the present problem on the flow pattern and the temperature distribution in terms of streamlines and isotherms in the boundary layer regime along the surface of the cylinder through figures 4 to 7. Following relations are considered to measure the
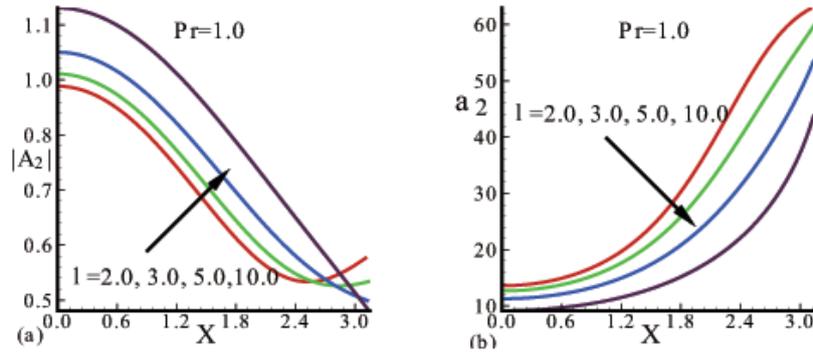
Figure 3. (a) Amplitude and (b) phase of heat transfer at Pr=1.0, $\omega = 0.5$, $\omega\tau = \pi/4$ while $\lambda = 2.0, 3.0, 5.0$ and 10.0.

values of oscillating stream function and oscillating temperature function.

$$\psi = \psi_s(X, Y) + \varepsilon(\cos \omega\tau \psi_i(X, Y) - \sin \omega\tau \psi_r(X, Y)) \tag{38}$$

$$G = G_s(X, Y) + \varepsilon(\cos \omega\tau G_i(X, Y) - \sin \omega\tau G_r(X, Y)) \tag{39}$$

In equation (38) ψ_s, ψ_r, and ψ_i are measured from the following expression:

$$\psi_s(X, Y) = \int_0^Y U_s(X, \chi) d\chi, \quad \psi_r(X, Y) = \int_0^Y U_r(X, \chi) d\chi, \\ \psi_i(X, Y) = \int_0^Y U_i(X, \chi) d\chi \tag{40}$$

Figure 4. Streamlines along a circular cylinder at Pr=1.0, $\omega = 1.0$, $\omega\tau = \pi/4$, $\varepsilon = 0.01$ for (a) $\lambda = 3.0$ and (b) $\lambda = 10.0$.
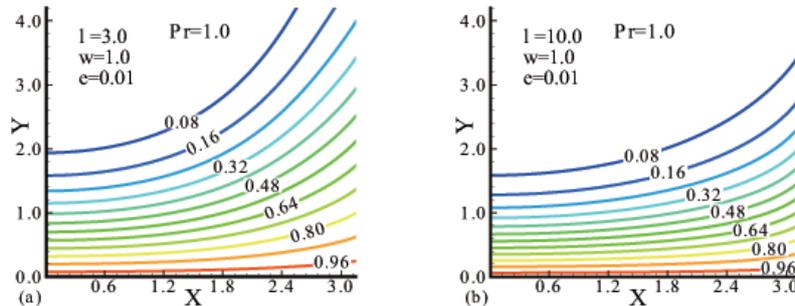

Figure 5. Isotherms along a circular cylinder at Pr=1.0, $\omega = 1.0$, $\omega\tau = \pi/4$, $\varepsilon = 0.01$ for (a) $\lambda = 3.0$ and (b) $\lambda = 10.0$.

Numerical solutions are obtained for Prandtl number, Pr=1.0, amplitude of oscillation, $\varepsilon = 0.01$, different values of mixed convection parameter λ and frequency of oscillation ω.

A comparisons of streamlines and isotherms for values of $\lambda = 3.0$ and 10.0 are shown in figures 4 and 5. From these figures one can observe that there is relatively a conspicuous change happens both for streamlines and isotherms. In figure 4, it is found that in upper surface $\psi_{max} = 19.53$ and in lower surface $\psi_{min} = 1.20$. Here the viscosity is minimum at the upper boundary and maximum at the lower boundary.

For $\lambda = 3.0$, the momentum boundary layer as well as thermal boundary layer become higher for which the flow rate stronger near the surface of the cylinders; on the other hand, for $\lambda = 10.0$, weaker flow is seen near the surfaces of the cylinder, since in this case both the momentum and thermal boundary layers become thinner. From the given isotherms one can see that, the fluid temperature is higher near the lower boundary and lower near the upper boundary. Nearly parallel isotherms in the upper part of the cell indicate that heat transport is almost entirely by conduction.

At the present stage, figures 6 and 7 provided the comparison between streamlines and isotherms, respectively in the same way as above for $\lambda = 2.0$, Prandtl number Pr=1.0, amplitude of oscillation, $\varepsilon = 0.01$ at $\omega\tau = \pi/4$ and for $\omega = 1.0, 4.0$ which designates the frequency of oscillation. It is apparent from these figures that there is relatively little but significance change in the streamlines and isotherms. When the curvature parameter X is increasing, then initially streamlines in terms of velocity field is decreasing. For $\omega = 1.0$, the momentum boundary layer becomes higher and we have a stronger flow. But for increasing the frequency of oscillation $i.e.$, for $\omega = 4.0$, the momentum boundary layer becomes thinner and we have a weaker flow in the downstream region. The flow remains almost symmetric about the vertical centerline.
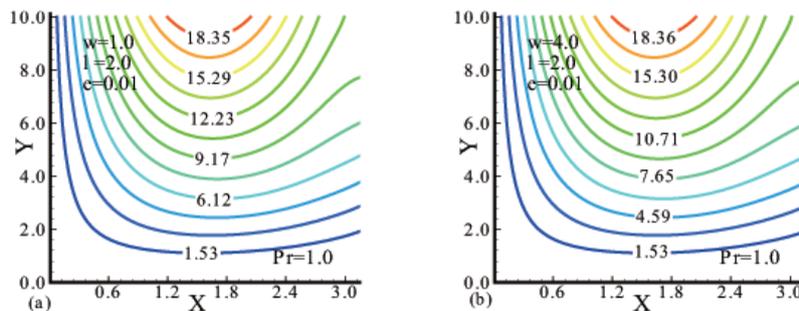

Figure 6. Streamlines along a circular cylinder at Pr=1.0, $\lambda = 2.0$, $\omega\tau = \pi/4$, $\varepsilon = 0.01$ for (a) $\omega = 1.0$ and (b) $\omega = 4.0$.
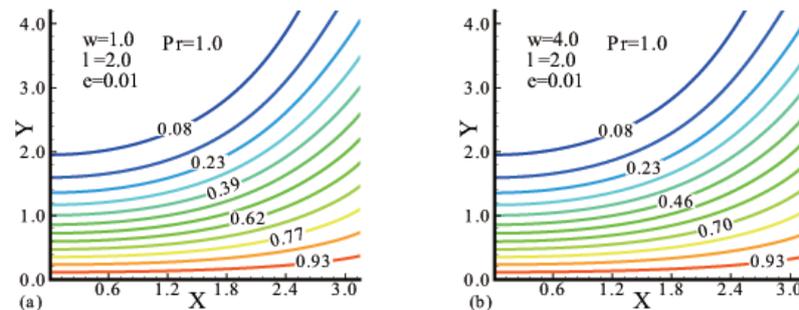

Figure 7. Isotherms along a circular cylinder at Pr=1.0, $\lambda = 2.0$, $\omega\tau = \pi/4$, $\varepsilon = 0.01$ for (a) $\omega = 1.0$ and (b) $\omega = 4.0$.

4.3 Effect of Physical Parameter on Transient Shear Stress and Heat Transfer

Numerical values of the transient shear stress, τ_w, and heat-transfer, q_w, against τ obtained from the formulas (32) and (33), which are presented graphically in figures through 8 and 9. Effect of the frequency term, ω and the values of mixed convection parameter λ on the improvement of transitory heat-transfer and skin-friction coefficients, for Pr = 1.0, $\omega\tau = \pi/4$ and $\varepsilon = 0.01$ are shown in the respective figures. In figures 8(a) and 8(b), numerical estimates of the changing heat-transfer and skin-friction coefficient versus the non-dimensional time function τ have been shown for $\lambda = 2.0, 5.0$ and 10.0. From these figures, it is observed that at every station of τ, owing to increase in the value of λ, leads to increase in the magnitude of the oscillating shear stress and an decrease in the oscillating

heat transfer coefficients. But the phase of oscillation is increasing in both phases constants on account of skin friction and heat transfer with the increasing values of λ. It is also remarked that amplitude oscillation is exceeding for transitory heat transfer constants than that of the transitory shear stress coefficients.
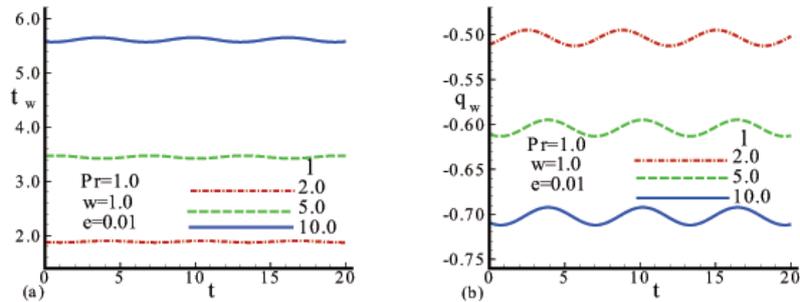

Figure 8. Transient (a) skin-friction coefficient and (b) heat transfer coefficient at Pr=1.0, $\omega = 1.0$, $\omega\tau = \pi/4$, $\varepsilon = 0.01$ for $\lambda = 2.0, 5.0$ and 10.0.
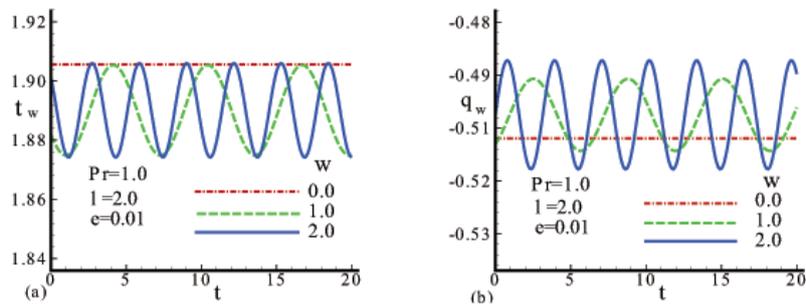

Figure 9. Transient (a) skin-friction coefficient and (b) heat transfer coefficient at Pr=1.0, $\lambda = 2.0$, $\omega\tau = \pi/4$, $\varepsilon = 0.01$ for $\omega = 0.0, 1.0$ and 2.0.

Now we are looking into the effect of change on the oscillating skin-friction and heat transfer from the surface. Effect of these geometric varieties taking the value of ω to be 0.0, 1.0 and 2.0 on the skin-friction and heat transfer are shown, respectively, in figures 9(a) and 9(b). In this regards Pr = 1.0, $\lambda = 2.0$ and $\varepsilon = 0.01$ at $\omega\tau = \pi/4$ have been taken. In these figures, one can see that when the frequency of oscillation ω increased magnitude of the skin friction get decreased and magnitude of the heat transfer get increased at every τ station. When $\omega = 0.0$ i.e there is no frequency of oscillation leads the amplitude of oscillation for both skin friction and heat transfer constants and graphically represent a straight line as shown in figures 9(a) and 9(b). Finally, amplitude of oscillation for both skin friction and heat transfer are increased with the increase of frequency of oscillation. This is expected since rise of frequency of the surface temperature should lead to increment the frequency of oscillation of the shear-stress and temperature of the fluid in the vicinity of the surface of the cylinders.

5. Conclusion

The analysis carried out here is concerned with two-dimensional mixed convection boundary value problem over a horizontal circular cylinder with oscillating surface temperature with time dependent velocity, which is immersed in a viscous incompressible fluid. We have attempted to find how the parameter λ and the frequency parameter ω affect both for steady and oscillating flow. Solutions of the transformed couple local non-similar boundary layer equations are integrated numerically employing the finite difference method. The steady state problem that was investigated by Merkin (1977) and Hossain et al. (1999) has been revisited by the aforementioned (DNS) method and our results are visually good well with the respective authors. The results of oscillating flow have been obtained in terms of amplitude and phase of local skin friction and rate of heat transfer with the change of the physical parameters, namely, λ, Pr, ω and ε. Effects of the identical parameters are also shown on the oscillating shear stress and surface rate of heat transfer as well as on the oscillating streamlines and isotherms. From this study we can draw the following conclusions:

- When the curvature parameter X increases, the amplitude of the skin friction decreases. Also amplitude of the skin friction rises remaining to increment in the values of mixed parameterλ. Phase angle α_1 decrease owing to increase for the parameters λ with the distance of the curvature X and has a phase lag.

- The amplitude $|A_2|$ increases with the rise of the parameter λ upto the upper stagnation point of the cylinder. Phase of oscillation α_2 are decreases owing to increase of the parameter λ upto the curvature $X = \pi$ and always has a phase lead.

- The viscosity is minimum at the upper boundary and maximum at the lower boundary. For $\lambda = 3.0$, the momentum boundary layer become higher for which the flow rate stronger and for $\lambda = 10.0$, weaker flow is seen near the surfaces of the cylinder, since in this case the momentum boundary layers become thinner.

- Isotherms show that, the temperature of the fluid is higher near the inferior and lower near the upper boundary.

- Increasing values of λ, leads to increase in the magnitude of the oscillating shear stress and an decrease in the oscillating heat transfer coefficients. Also amplitude of oscillation for both skin friction and heat transfer are increased with the increase of frequency of oscillation.

Nomenclature

R	Radius of the cylinder
g	Acceleration due to gravity
C_p	Specific heat at constant pressure
Gr	Grashof number
Re	Reynolds number
Pr	Prandtl number
q_w	Surface rate of heat transfer
T	Temperature of the fluid in the boundary layer
T_∞	Temperature of the ambient fluid
T_w	Temperature of the heated surface
ΔT	Temperature difference, $T_w - T_\infty$
G	Dimensionless temperature funcion
u, v	Dimensional fluid velocities in the x- and y- direction, respectively
U, V	Dimensionless fluid velocities in the X- and Y- direction, respectively
x, y	Coordinates measuring distance round and normal to the cylinder, respectively
X, Y	Dimensionless coordinates measuring distance round and normal to the cylinder, respectively
U_∞	Free stream velocity
U_e	External velocity
t	Time
τ_w	Dimensionless shear-stress

Greek letters

ψ	Stream function
κ	Thermal conductivity of the fluid
β	Coefficient of thermal expansion
λ	Mixed convection parameter
ω	Frequency of oscillation
ε	Amplitude of oscillation
ν	Kinematic viscosity
τ	Dimensionless time
ρ	Density of the fluid

Subscripts-Superscripts

w	Surface conditions
∞	Ambient condition

s	Steady component
o	Unsteady component
$'$	Differentiation with respect to Y

Acknowledgment

References

Acrivos, A. (1966). On the combined effect of forced and free convection heat transfer in laminar boundary layer flows. *J. Chem. Engng. Sci., 21*, 343-352. http://dx.doi.org/10.1016/0009-2509(66)85027-3

Aldoss, T. K., Ali, Y. D., & Al-Nimr, M. A. (1996). MHD mixed convection from a horizontal circular cylinder. *Num. Heat Transfer, Part A., 30*, 379-396. http://dx.doi.org/10.1080/10407789608913846

Amin, N., & Riley N. (1995). Mixed convection at a stagnation point. *Q. J. Mech. Appl. Math., 48*, 111-121. http://dx.doi.org/10.1093/qjmam/48.1.111

Glauert, M. B., & Lighthill, M. J. (1995). The axisymmetric boundary layer on a long thin cylinder. *Proc.Roy. Soc. London, Ser. A, 230*, 188-203. http://dx.doi.org/10.1098/rspa.1955.0121

Gorla, R. S. R. (1979). Unsteady viscous flow in the vicinity of an axisymmetic stagnation point on a circular cylinder. *Int. J. Engineering Science., 17*, 87-93. http://dx.doi.org/10.1016/0020-7225(79)90009-0

Hossain, M. A., Kamrujjaman, M., & Gorla, R. S. R. (2009). Fluctuating free convection flow along heated horizontal circular cylinders. *Int. J. Fluid Mech. Res., 36*, 207-230. http://dx.doi.org/10.1615/InterJFluidMechRes.v36.i3.20

Hossain, M. A., Hussain, S., & Rees, D. A. S. (2001). Influence of fluctuating surface temperature and concentration on natural convection flow form a vertical flat plate. *ZAMM, 81*, 699-709.

Hossain, M. A., Das, S. K., & Pop, I. (1998). Heat transfer response of MHD free convection flow along a vertical plate to surface temperature oscillations. *Int. J. Non-Linear Mechanics, 33*, 541-553. http://dx.doi.org/10.1016/S0020-7462(96)00151-5

Hossain, M. A., Kutubuddin, M., & Pop, I. (1999). Radiation-conduction interaction on mixed convection from a horizontal circular cylinder. *Heat and Mass Transfer., 35*, 307-314. http://dx.doi.org/10.1007/s002310050329

Lighthill, M. J. (1954). The response of laminar skin friction and heat transfer to fluctuations in the stream velocity. *Proc.Roy. Soc. London, Ser. A, 224*, 1-23. http://dx.doi.org/10.1098/rspa.1954.0137

Lin, F. N., & Chao, B. T. (1974). Laminar free convection over two-dimensional and axisymmetric bodies of arbitrary contour. *J. Heat Transfer, Trans. ASMF. Series C, 96*, 435-442. http://dx.doi.org/10.1115/1.3450223

Merkin, J. H. (1967). Oscillatory free convection from an infinite horizontal cylinder. *J. Fluid Mech., 30*, 561-575. http://dx.doi.org/10.1017/S0022112067001612

Merkin, J. H. (1977). Mixed convection from a horizontal circular cylinder. *Int. J. Heat and Mass Transfer., 20*, 73-77. http://dx.doi.org/10.1016/0017-9310(77)90086-2

Ramachandran, N., Chen, T. S., & Armaly, B. F. (1988). Mixed convection in stagnation flows adjacent to vertical surfaces. *ASME J. Heat Trans., 110*, 373-377. http://dx.doi.org/10.1115/1.3250494

Seshadri, R., Sreeshylan, N., & Nath, G. (2002). Unsteady mixed convection flow in the stagnation region of a heated vertical plate due to impulsive motion. *J. Heat Mass Trans., 45*, 1345-1352. http://dx.doi.org/10.1016/S0017-9310(01)00228-9

Copyrights